IOPscience iopscience.iop.org

Home Search Collections Journals About Contact us My IOPscience

Phonon-assisted tunnelling as a process determining current dependence on field and temperature in MEH-PPV diodes

This article has been downloaded from IOPscience. Please scroll down to see the full text article.

2005 J. Phys.: Condens. Matter 17 4147

(http://iopscience.iop.org/0953-8984/17/26/013)

View the table of contents for this issue, or go to the journal homepage for more

Download details:
IP Address: 129.252.86.83
The article was downloaded on 28/05/2010 at 05:12

Please note that terms and conditions apply.

INSTITUTE OF PHYSICS PUBLISHING JOURNAL OF PHYSICS: CONDENSED MATTER

J. Phys.: Condens. Matter **17** (2005) 4147–4155 doi:10.1088/0953-8984/17/26/013

Phonon-assisted tunnelling as a process determining current dependence on field and temperature in MEH-PPV diodes

P Pipinys and A Kiveris[1]

Department of Physics VPU, Studentu 39, Vilnius 08106, Lithuania

E-mail: studsk@vpu.lt

Received 17 March 2005, in final form 10 May 2005
Published 17 June 2005
Online at stacks.iop.org/JPhysCM/17/4147

Abstract
In this paper we would like to show the applicability of phonon-assisted tunnelling theories for explanation of temperature-dependent current–voltage (I–V) characteristics of diodes based on organic thin films of conjugated polymers, such as poly[2-methoxy, 5-(2′-ethyl-hexyloxy)-1,4-phenylene-vinylene] (MEH-PPV). For this purpose the I–V characteristics measured for MEH-PPV by Campbell *et al* (1997 *J. Appl. Phys.* **82** 6326), Lupton and Samuel (1999 *J. Phys. D: Appl. Phys.* **32** 2973), and van Woudenbergh *et al* (2001 *Appl. Phys. Lett.* **79** 1697) are compared with the free carrier generation rate dependence on field strength using the phonon-assisted tunnelling theories. A strong dependence of charge carrier mobility on temperature is also explained by this model. The presented model allows us not only to explain the temperature variation of I–V and mobility data, but also to estimate the density of traps taking part in the current flow.

1. Introduction

Despite extensive investigation of conduction in π-conjugated polymers, which are materials for applications in organic light-emitting diodes (LEDs), the charge carrier transport mechanism is not well understood. Most frequently space charge limited current (SCLC) models, both without traps and including trapping processes, have been used to explain the mechanism of carrier transport in these materials [1–8].

In the absence of trapping and if the charge carrier mobility is field independent the SCLC model predicts the well known square-law dependence of current density J on applied voltage V ($J \sim V^2$) [9, 10]. The experimental I–V data often show much higher power law characteristics (e.g. $I \sim V^8$). Such types of characteristics are attributed to the filling of

[1] Author to whom any correspondence should be addressed.

 © 2005 IOP Publishing Ltd Printed in the UK

traps with a certain distribution in energy space, or to the electric field enhancement in the carrier mobility [11–16]. The origin of the mobility field enhancement is attributed to the Frenkel–Poole process [17] or to the tunnelling of carriers through the localized states.

However, these models often meet difficulties when seeking a quantitative agreement with experimental data. For example, Campbell *et al* [3] have measured the current–voltage characteristics in the wide temperature range of 270–30 K. At high fields ($V/d > 5 \times 10^5$ V cm^{-1}) J–V curves at different temperatures for single-layer polymer LEDs of PPV were fitted to the power law of the form $J = V^m$, where m increased with decreasing temperature. The results were explained by SCLS models involving an exponential trap distribution or hopping transport field and temperature dependent mobility [4]. But both the models could not explain the observed temperature dependence of m and the abrupt change of slope in the J–V characteristics with increased bias.

Kapoor *et al* [18] have reinterpreted these results on the assumption that the charge carrier transport mechanism needed to describe the low-temperature data is different from that applicable to high-temperature data. The authors of [18] have explained the high-temperature data on the basis of the improved trapping model. With a set of chosen parameters the good fit of the model with J–V data was obtained only at 270 K and for bias >5 V. For the curves at lower temperatures other values of mobility were taken. Below 190 K the discrepancy between the calculated and experimental curves increased very rapidly. Therefore, at low temperatures the J–V characteristics were explained using the mobility model. Fitting of the model to the experimental curves at lower temperatures (from 190 to 30 K) was performed using different trap densities for results at different temperatures.

Lupton and Samuel [19, 20] have explained the temperature-dependent J–V data for polymer LEDs based on conjugated polymer MEH-PPV by the model, which includes both injection and transport [21]. Good agreement with the experiment was found using strongly field- and temperature-dependent mobility. However, for each temperature different values of fitting parameters (the barrier height to injection, zero-field mobility, and field dependence mobility) must be applied. Thus the curves were fitted independently from each other over a temperature range from 100 to 280 K. A good fit was obtained for the J–V curve measured at 280 K, but there was a deviation at lower temperatures and for low field strengths.

Some investigators [22–25] involved carrier-tunnelling processes for the explanation of light emitting characteristics and carrier transport in polymer LED devices. Parker [22] has suggested that characteristics of LEDs based upon MEH-PPV are determined by tunnelling of both the holes and electrons through interface barriers caused by the band offset between the polymer and the electrodes. He explained measured I–V characteristics by Fowler–Nordheim (FN) tunnelling of electrons/holes through a triangular-shaped barrier at the electrode. For explanation of the temperature dependence of the I–V characteristics thermionic emission was cited. It is worth mentioning that the FN tunnelling for injection in [19] was rejected on the ground that the tunnelling barrier predicted by a simple FN analysis increases by more than a factor of two from 0.2 to 0.45 eV as the LED is cooled from room temperature to 13 K, while the fitted barrier height to the injection hole from the ITO anode was found to lower from 0.58 eV at 300 K to 0.41 eV at 100 K.

It is evident that interpretation of experimental data on carrier transport in polymers appears to vary among different investigators, but in all cases the same models or their modifications such as for the explanation of current at high field in the inorganic materials are involved. Therefore, in this paper we present an alternative explanation of temperature-dependent I–V characteristics in some organic films on the assumption that these dependences are caused by temperature- and field-dependent charge carriers tunnelling from localized states to conducting ones as a process whose mechanism is phonon-assisted tunnelling [26–28]. The tunnelling

processes, as shown above, were invoked by several investigators for explanation of some peculiarities of temperature dependent I–V data in organic materials, but these attempts were not very successful because FN tunnelling is essentially a temperature-independent process. The phonon-assisted tunnelling theories predict an absorption/emission of phonons in the process of charge carrier tunnelling. For this reason the tunnelling becomes a temperature-dependent process and might be taken into account for explaining the temperature-dependent I–V data measured in organic materials.

2. Theory and a comparison with experimental data

The quantum mechanical tunnelling theories, accounting for interaction of electrons with phonons, were proved to be efficient in describing centre ionization in inorganic devices [29, 30]. Recently, it has been shown that the phonon-assisted tunnelling model can explain temperature-dependent I–V characteristics for polyethylene and other insulating polymers [31]. In the present paper we apply this model to describe the temperature-dependent I–V data obtained for devices on the basis of PPV derivatives. We will compare the temperature-dependent I–V characteristics of MEH-PPV films extracted from [3, 19] with the transition rate of an electron/hole from centre to conducting state dependence on field strength and temperature, which follows from phonon-assisted tunnelling theory. For this purpose the equation derived in [26] for electron tunnelling with phonon participation from the deep centre to the conduction band is used:

$$W_T = \frac{eE}{(8m^*\varepsilon_T)^{1/2}}[(1+\gamma^2)^{1/2} - \gamma]^{1/2}[1+\gamma^2]^{-1/4} \exp\left\{-\frac{4}{3}\frac{(2m^*)^{1/2}}{eE\hbar}\varepsilon_T^{3/2} \times [(1+\gamma^2)^{1/2} - \gamma]^2[(1+\gamma^2)^{1/2} + \tfrac{1}{2}\gamma]\right\}, \qquad (1)$$

where

$$\gamma = \frac{(2m^*)^{1/2}\Gamma^2}{8e\hbar E\varepsilon_T^{1/2}}. \qquad (2)$$

Here $\Gamma^2 = 8a(\hbar\omega)^2(2n+1)$ is the width of the centre absorption band caused by interaction with longitudinal optical phonons, $n = [\exp(\hbar\omega/(k_B T)) - 1]^{-1}$, where $\hbar\omega$ is a phonon energy, ε_T is the energetic depth of the centre, e is the electron charge, and a is the electron–phonon interaction constant ($a = \Gamma_0^2/8(\hbar\omega)^2$). In the case of weak electron–phonon interaction ($\gamma \to 0$) expression (1) has a similar form as that obtained by Franz [32].

Assuming that the current I through a polymer layer is proportional to the charge carrier tunnelling rate $W_T(E, T)$ from a set of energy levels (traps) to the conducting states, W being a function of temperature T and field strength E, we will compare the measured temperature dependent I–V data of MEH-PPV polymer film extracted from figure 4(a) in [3] with the tunnelling rate dependence on field strength and temperatures at which the measurements were fulfilled.

The fit of computed $W_T(E, T)$ dependences carried out for different temperatures with experimental data is shown in figure 1. The calculation was performed using the electron effective mass value $m^* = 1.2\ m_e$; for the phonon energy the value of 0.034 eV was taken. The electron–phonon coupling constant a was chosen so that the best fit of the experimental data with the calculated dependences should be received. The value of centre depth (activation energy) ε_T was evaluated from the plot of $\ln I$ versus $1/T$ at 1 V of the results in figure 1. The comparison shows a good agreement of the experimental data with calculated curves in all the temperature range.

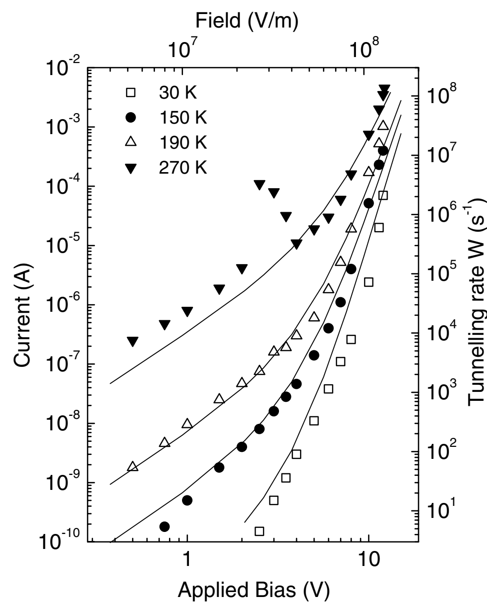

Figure 1. I–V characteristics of a sample MEH-PPV with thickness of 94 nm at different temperatures from [3, figure 4(a) (symbols)] fitted to the theoretical tunnelling rate $W_T(E, T)$ dependences (solid lines) calculated for the same temperatures as the experimental data using the following parameters: $a = 5.4$, $\varepsilon_T = 0.58$ eV, $m^* = 1.2\, m_e$, $\hbar\omega = 0.034$ eV.

On the basis of this model a nonlinear behaviour of the Arrhenius plot (ln J versus $1/T$) is comprehensible because it is predetermined by the theory. It is worth noting that non-linearity of these plots, which determines the variation of energy activation from 0.6 eV at high temperatures to about 0.02 eV at low temperatures, was the main reason that Kapoor *et al* have suggested two different mechanisms of current at different (high and low) temperatures, namely, the improved trapping model at near room temperature and the hopping mobility model at low temperatures [18].

In figure 2 the theoretical dependences ln $W(E, T)$ versus $1/T$ for different field strength are shown. Symbols upon the curves represent experimental values of the current extracted from figure 4(a) in [3] for the same field strength as the theoretical ones. It is seen that the variation of the slope for the theoretical curves in the Arrhenius plot and the experimental data is the same, i.e., the slope of the curves both for the theoretical and experimental dependences regularly increases as the temperature decreases. Still more, the theory gives the same variation for ln $W(E, T)$ versus $1/T$ dependences with field strength as was obtained for the experimental data. Both these circumstances give a strong confirmation of the presented model.

If electrons/holes released from traps dominate the current in a device then the current value I may be expressed by the equation [33]

$$I = (1/2)AeNW_T, \tag{3}$$

where A is the effective generation volume (for these specimens thickness being 94 nm, $A = 10^{-7}$ cm^3) and N is the trap density. Substituting the current value I and corresponding value W from figure 1 to relation (3), we obtain $N \sim 4 \times 10^{15}$ cm^{-3}. This value is in reasonable agreement with the value of $\sim 10^{16}$ cm^{-3} determined by the authors [3] by a different procedure.

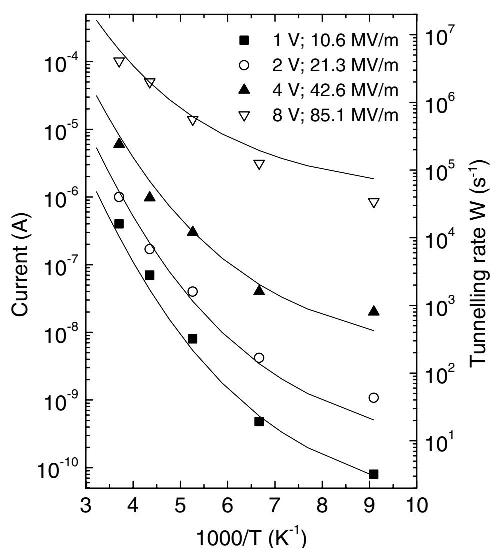

Figure 2. Experimental values of I from figure 1 plotted as a function of reciprocal temperature $1/T$ for applied bias $V = 1, 2, 4$ and 8 V (symbols) fitted to $W_T(E, T)$ against $1/T$ dependences (solid lines) calculated for the E corresponding to the experimental $E = V/d$ values. The other parameters are the same as for figure 1.

In figure 3 the J–V data from [19] for a single carrier MEH-PPV polymer LED are presented. For these devices the fact was ascertained that current is actually symmetric in low forward and reverse biases. This implies that current is bulk limited and is most likely due to transport through impurity levels in the material, that is the case when the experimental data were often described by the Poole–Frenkel emission mechanism; however, we will explain these data using quantum mechanical tunnelling theory.

Figure 3(a) shows the fit of these data performed by the authors of [19] to their device model based on the classical physics approach. We want to emphasize that the fit of data with their model is performed using temperature-dependent fitting parameters, including the barrier height for injection. In figure 3(b) the experimental data are compared with the $W(E, T)$, calculated according to equation (1) using the same set of parameters for all measured temperatures. It can be seen that the theoretical curves in this case fit well to the experimental data in the whole range of field strengths. Trap density, as determined using equation (3) (for $A = 1.65 \times 10^{-5}$ cm^3) and results from figure 3(b), is equal to 3×10^{15} cm^{-3}.

We want to mention that the fit of measured J–V data with the calculated current densities presented in figure 3(a) was performed in [19] using field-dependent mobility of the form

$$\mu_{(E)} = \mu_{(E=0)} \exp(\surd(E/E_0)), \tag{4}$$

where $\mu_{(E=0)}$ is the zero-field mobility.

The temperature dependence of fitting parameters, i.e. $\mu_{(E=0)}$, E_0 and the barrier height, were deduced in [19] from measured current–voltage characteristics. The variation of the $\mu_{(E=0)}$ parameter with temperature is shown in figure 4. It is seen that this parameter varies exponentially with inverse temperature and decreases by 12 orders of magnitude between 300 and 140 K. The authors of [19] related such behaviour of this parameter to the characteristics of hopping transport. However, below 140 K the data appeared to diverge from the predicted straight-line relationship. If the current is governed by the charge carrier generation process

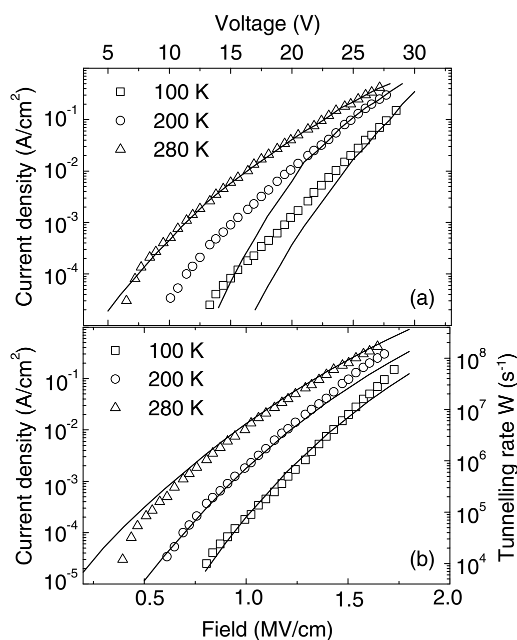

Figure 3. Experimental J–V characteristics for the MEH-PPV LEDs (film thickness of 165 nm) from [19, figure 7 (symbols)]. Solid lines represent the simulated best fit: (a) performed by the authors of [19] to their model using for each curve different values of fitting parameters, $T = 280$ K, barrier height $\varphi_b = 0.54$ eV, $\mu_{(E=0)} = 3.9 \times 10^{-6}$ cm^2 V^{-1} s^{-1}, $E_0 = 1.9 \times 10^5$ V cm^{-1}; $T = 200$ K, $\varphi_b = 0.44$ eV, $\mu_{(E=0)} = 6.7 \times 10^{-12}$ cm^2 V^{-1} s^{-1}, $E_0 = 7.3 \times 10^3$ V cm^{-1}; $T = 100$ K, $\varphi_b = 0.41$ eV, $\mu_{(E=0)} = 1.1 \times 10^{-18}$ cm^2 V^{-1} s^{-1}, $E_0 = 1.9 \times 10^3$ V cm^{-1}; (b) to the theoretical $W_T(E, T)$ dependences calculated using for different temperatures the same set of parameters, $a = 4.7$, $\varepsilon_T = 0.58$ eV, $m^* = 1.2\, m_e$, $\hbar\omega = 0.034$ eV.

then the mobility dependence on temperature will be the same as for current. In figure 4 curves represent the temperature dependence of ln W versus $(1/T)$ computed for three values of phonon energy and fitted to the ln $\mu_{(E=0)}$ versus $(1/T)$ dependence. The solid curve calculated for the phonon energy of 34 meV matches well the temperature variation of the $\mu_{(E=0)}$ parameter. The temperature at which the bending in these dependences occurs depends on the value of phonon energy and this allows estimation of the energy of the phonon taking part in the tunnelling process.

The dependence of mobility on temperature also exhibits similar behaviour. Figure 5 shows the temperature dependence of the hole mobility in PAPPV film measured at two values of field strength represented from [34]. For $T > 150$ K the temperature dependence of the hole mobility obeyed a ln μ versus T^{-2} law but in the lower temperature region the temperature dependence was weaker. These mobility dependences multiplied by field strength in figure 5 are fitted to ln W versus $1/T$ dependences. The fit of experimental data with computed tunnelling rate dependence on reciprocal temperature is very good in the whole temperature range. Thus, phonon-assisted carrier tunnelling from traps controls both the current and carrier mobility.

Finally, in figure 6 the temperature-dependent I–V characteristics obtained by van Woudenbergh *et al* [35] for an ITO/Ag/PPV/Ag and for an ITO/PPV/Al device are fitted with our model. In these devices injection-limited current (ILC) was obviously observed with different barrier heights for carrier injection from Ag ($\varphi_b = 0.95$ eV) and Al ($\varphi_b = 1.05$ eV) electrodes.

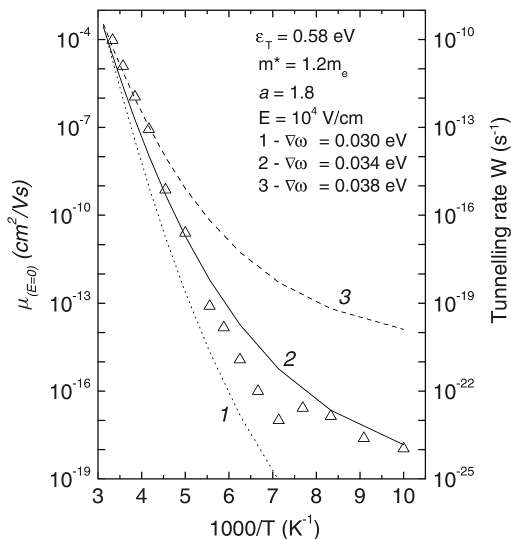

Figure 4. Variation of the zero-field mobility $\mu_{(E=0)}$ with the temperature from [19, figure 8 (symbols)] fitted to $\ln W_T$ dependences versus $1/T$ computed for $\hbar\omega = 0.034$ eV (solid curve), $\hbar\omega = 0.030$ eV (dotted curve) and $\hbar\omega = 0.038$ eV (dashed curve). The values of W are given for curve (2) only.

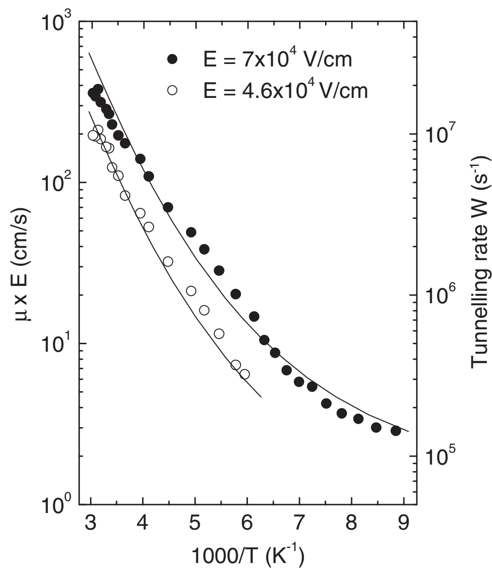

Figure 5. Temperature dependence of the mobility multiplied by the field strength from [34] (symbols) fitted to $W_T(E, T)$ versus $1/T$ dependences (solid curves) using the following parameters: $a = 7$, $\varepsilon_T = 0.48$ eV, $m^* = 1.2\, m_e$, $\hbar\omega = 0.034$ eV.

The model offered by the authors of [35] '…in which the spread in the charge transporting site energy due to disorder is taken into account, consistently describes the measured field and temperature dependence of the injection process. However, at higher fields (1.2×10^8 V m^{-1}) the experimental data show stronger field dependence as compared to the theoretical predictions'.

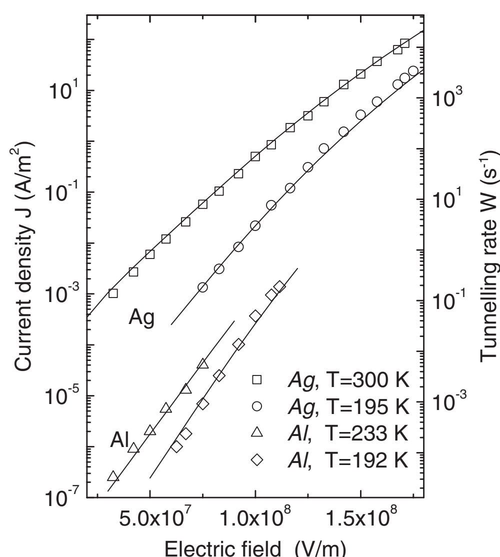

Figure 6. Current density J versus electric field for an ITO/Ag/PPV/Ag and an ITO/PPV/Al device at different temperatures extracted from [35] (symbols) fitted to the calculated $W_T(E, T)$ versus E dependences (solid lines). The calculation was performed using the following parameters: $a = 4$, $m^* = 1.2\ m_e$, $\hbar\omega = 0.054$ eV, $\varepsilon_T = 0.95$ eV (for the Ag electrode) and $\varepsilon_T = 1.05$ eV (for the Al electrode).

In figure 6 these experimental data are fitted to computed $W(E, T)$ dependences. As is seen, the theoretical curves over the entire range of field strengths fit very well for both devices to the experimental data. It should be noted that the comparison between experimental data and theory is performed using for both devices the same values of phonon energy, strength of phonon–electron interaction, and effective mass of carriers. This suggests that the tunnelling processes which determine the temperature and field dependence of the current occur from the localized states of PPV. The difference in value of barrier height for these devices may be explained by the assumption that charge carrier injection occurs from the Fermi level of the electrode into tail states of the exponentional distribution of localized states [4] in the interface layer between metal and polymer ($\varepsilon_T = 0.95$ eV for Ag and $\varepsilon_T = 1.05$ eV for Al electrodes).

The second step which determines current dependence on bias and temperature is phonon-assisted tunnelling of localized charge carriers to the conducting state of the polymer.

If there is no significant re-capture of carriers, the current density will be determined as $J = eN_s W_T$, where N_s is the filled state density. From the results in figure 6, the derived value of N_s is found to be $\sim 5 \times 10^{12}$ cm^{-2}.

3. Conclusions

We have shown that the model based on the phonon-assisted tunnelling, as a free carrier generation process, is able to describe the temperature- and field-dependent current–voltage characteristics of diodes on the basis of PPV derivatives. An advantage of this model over the mentioned SCLC with hopping type field and temperature-dependent charge carrier mobility model is hidden in the possibility to describe the behaviour of I–V data measured at both high and low temperatures with the same set of parameters characterizing the material (see the caption for figure 3). Phonon-assisted tunnelling is the only mechanism that explains the

nonlinear dependence of ln I versus $1/T$ at high fields. On the basis of this model the variation of charge carrier mobility with temperature is explained as well. Since the peculiarities of the carrier mobility variation with temperature, as seen from figure 4, strongly depend on phonon energy, this allows estimation of the energy value of phonons taking part in the tunnelling process. Assuming the domination of current flow by the process of phonon-assisted tunnelling of electrons from traps to the conducting states enables us to determine the density of traps participating in a current flow.

References

[1] Bloom P W M, de Jong M J M and Vleggaar J J M 1996 *Appl. Phys. Lett.* **68** 3308

[2] Burrows P E, Shen Z, Bulovic V, McCarty D M, Forrest S R, Cronin J A and Thompson M E 1996 *J. Appl. Phys.* **79** 7991

[3] Campbell A J, Bradley D D C and Lidzey D G 1997 *J. Appl. Phys.* **82** 6326

[4] Campbell A J, Weaver M S, Lidzey D G and Bradley D D C 1998 *J. Appl. Phys.* **84** 6737

[5] Lee C H, Kang G W, Jeon J W, Song W J, Kim S Y and Seoul C 2001 *Synth. Met.* **117** 75

[6] Kang H S, Kim K H, Kim M S, Park K T, Kim K M, Lee T H, Lee C Y, Joo J, Lee D W, Hong Y R, Kim K, Lee G J and Jin J-I 2002 *Synth. Met.* **130** 279

[7] Shen J and Yang J 1998 *J. Appl. Phys.* **83** 7706
Yang J and Shen J 1999 *J. Appl. Phys.* **85** 2699

[8] Nikitenko V R, Heil H and von Seggern H J 2003 *J. Appl. Phys.* **94** 2480

[9] Mott N F and Davis E A 1971 *Electronic Processes in Non-Crystalline Materials* (Oxford: Clarendon)

[10] Kao K C and Hwang W 1981 *Electrical Transport in Solids* (Oxford: Pergamon)

[11] Schein L B, Peled A and Glatz D 1989 *J. Appl. Phys.* **66** 686

[12] Dunlap D H, Parris P E and Kenkre V M 1996 *Phys. Rev. Lett.* **77** 542

[13] Blom P W M, de Jong M J M and von Munster M G 1997 *Phys. Rev.* B **55** R656

[14] Blom P W and Vissenberg M C J M 1998 *Phys. Rev. Lett.* **80** 3819

[15] Street R A, Knipp D and Völkel A R 2002 *Appl. Phys. Lett.* **80** 1658

[16] Schön J H and Batlogg B 2001 *J. Appl. Phys.* **89** 336

[17] Frenkel J 1938 *Phys. Rev.* **54** 647

[18] Kapoor A K, Jain S C, Poortmans J, Kumar V and Mertens R 2002 *J. Appl. Phys.* **92** 3835

[19] Lupton J M and Samuel I D W 1999 *J. Phys. D: Appl. Phys.* **32** 2973

[20] Lupton J M and Samuel I D W 2000 *Synth. Met.* **111/112** 381

[21] Davids P S, Campbell I H and Smith D L 1997 *J. Appl. Phys.* **82** 6319

[22] Parker I D 1994 *J. Appl. Phys.* **75** 1656

[23] Wolf U, Arkhipov V I and Bässler H 1999 *Phys. Rev.* B **59** 7507

[24] Tu N R and Kao K C 1999 *J. Appl. Phys.* **85** 7267

[25] Lee Ch, Park J-Y, Park Y-W, Ahn Y-H, Kim D-S, Hwang D-H and Zyung T-H 1999 *J. Korean Phys. Soc.* **35** S291

[26] Kiveris A, Kudžmauskas Š and Pipinys P 1976 *Phys. Status Solidi* a **37** 321

[27] Dalidchik F I 1978 *Zh. Eksp. Teor. Fiz.* **74** 472
Dalidchik F I 1978 *Sov. Phys.—JETP* **47** 247 (Engl. Transl.)

[28] Makram-Ebeid S and Lannoo M 1982 *Phys. Rev.* B **25** 6406

[29] Brazis R, Pipinys P, Rimeika A and Lapeika V 1990 *J. Mater. Sci. Lett.* **9** 266

[30] Pipinys P, Pipinienė A and Rimeika A 1999 *J. Appl. Phys.* **86** 6875

[31] Pipinys P, Rimeika A and Lapeika V 2004 *J. Phys. D: Appl. Phys.* **37** 828

[32] Franz W 1956 *Handbook of Physics* vol 17 (Berlin: Springer) p 155

[33] Migliorato P, Reita C, Tallarida G, Quinn M and Fortunato G 1995 *Solid-State Electron.* **38** 2075

[34] Barth S, Bässler H, Hertel D, Nikitenko V I and Wolf U 1999 *Pure Appl. Chem.* **71** 2067

[35] Van Woudenbergh T, Blom P W M, Vissenberg M C J M and Huiberts J N 2001 *Appl. Phys. Lett.* **79** 1697